Acteoside alleviates dextran sulphate sodium-induced ulcerative colitis via regulation of the HO-1/HMGB1 signaling pathway

WENJUAN GUO[1], XIAODI WANG[1], FANG LIU[1], SHUO CHEN[1], SHUAI WANG[1], QINGRUI ZHANG[1], LAN YUAN[2] and SHIYU DU[1]

[1]Department of Gastroenterology, China-Japan Friendship Hospital, Beijing 100029; [2]Peking University Medical and Health Analysis Center, Peking University Health Science Center, Beijing 100191, P.R. China

Received April 9, 2022; Accepted September 2, 2022

DOI: 10.3892/mmr.2022.12877

Abstract. Ulcerative colitis (UC) is a significant burden on human health, and the elucidation of the mechanism by which it develops has potential for the prevention and treatment of UC. It has been reported that acteoside (ACT) exhibits strong anti-inflammatory activity. In the present study, it was hypothesized that ACT may exert a protective effect against UC. The effects of ACT on inflammation, oxidative stress and apoptosis were evaluated using dextran sulphate sodium (DSS)-treated mice and DSS-treated human colorectal adenocarcinoma Caco-2 cells, which have an epithelial morphology. The results demonstrated that the ACT-treated mice with DSS-induced UC exhibited significantly reduced colon inflammation, as demonstrated by a reversal in body weight loss, colon shortening, disease activity index score, inflammation, oxidative stress and colonic barrier dysfunction. Further *in vivo* experiments demonstrated that ACT inhibited DSS-induced apoptosis in colon tissues, as demonstrated by the results of the TUNEL assay and the altered protein expression levels of Bax, cleaved caspase-3 and Bcl-2. Furthermore, DSS significantly stimulated the protein expression levels of high mobility group box 1 protein (HMGB1), which serves a central role in the initiation and progression of UC, an effect which was markedly inhibited by ACT. Finally, DSS significantly decreased the protein expression levels of heme oxygenase-1 (HO-1) in colon tissues and the effect of ACT on GSH, apoptotic proteins and HMGB1 was markedly attenuated in the presence of the HO-1 inhibitor tin protoporphyrin. In conclusion, ACT ameliorated colon inflammation through HMGB1 inhibition in a HO-1-dependent manner.

Correspondence to: Dr Shiyu Du, Department of Gastroenterology, China-Japan Friendship Hospital, 2 Yinghua East Road, Chaoyang, Beijing 100029, P.R. China
E-mail: dshiyudu@163.com

Key words: acteoside, ulcerative colitis, high mobility group box 1 protein, heme oxygenase-1

Introduction

Inflammatory bowel diseases (IBDs) are immune disorders that cause chronic inflammation in the gastrointestinal tract, and include ulcerative colitis (UC) and Crohn's disease (CD) (1-3). UC is limited to the colon and consists of diffuse mucosal inflammation, whereas CD can involve inflammation of any part of the gastrointestinal tract (4,5). It has been reported that China had the highest incidence of IBD in Asia in recent years (6).

Numerous studies have reported that inflammation, apoptosis, genetics, immune dysregulation and stress participate in the development of UC (3,7-10). Among these causes, apoptosis is considered to serve a critical role in the pathogenesis of UC and multiple strategies have been developed to treat IBD through the targeting of apoptosis. For example, it has been reported that maggot extracts (11), conjugated linoleic acid (12) and oxymatrine (13) can inhibit the initiation and progression of IBD. Mechanistic analysis has demonstrated that these compounds exert their protective effects through the inhibition of oxidative stress and inflammation in UC (11-13).

Acteoside (ACT) is a lipase inhibitor and a major component of *Ligustrum purpurascens* (kudingcha tea) (14). ACT has been reported to regulate inflammation and immune responses (15,16). For example, it has been reported that ACT inhibits the IL-1β-induced inflammation and apoptosis of chondrocytes through inhibition of Janus kinase/STAT, thereby protecting against surgery-induced osteoarthritis (17). Another study reported that ACT inhibits lipopolysaccharide (LPS)-induced inflammation in acute lung injury via regulation of the NF-κB signaling pathway (18). Hausmann *et al* (19) reported that ACT may ameliorate intestinal inflammation in a dextran sulphate sodium (DSS)-induced colitis model. However, the underlying mechanism via which ACT exerts a protective role remains largely unknown. The present study evaluated the mechanism underlying the protective effect of ACT in UC.

Materials and methods

Mice. All experiments were performed according to the Institutional Guidelines for the Care and Use of Laboratory Animals in Research (20) and were approved

by the Biomedical Ethics Committee of Peking University (approval no. LA2020356; Beijing, China). The 8-week-old C57BL/6 male mice (weight, 20-24 g; n=24) were obtained from the Department of Laboratory Animal Science, Peking University Health Science Center. The mice were housed at a temperature of 18-22˚C and a relative humidity of 50-60%. All mice had free access to food and water, and were maintained under a fixed 12-h light/dark cycle.

Induction and evaluation of UC. Mice were randomly divided into four groups as follows (n=6 per group): i) Control; ii) DSS; iii) DSS + 30 mg/kg ACT; and iv) DSS + 60 mg/kg ACT. Mice were treated with drinking water containing 4% DSS (FUJIFILM Wako Pure Chemical Corporation) to induce UC (21,22). Mice had no restriction on the dose of DSS solution for 7 consecutive days and control mice received standard drinking water throughout the 7 days of the experiment. ACT (Fig. 1A; CAS 61276-17-3; Shanghai Aladdin Biochemical Technology Co., Ltd.) was administered intraperitoneally (i.p.) every day for 7 consecutive days (the same days the mice were given DSS). The body weight of the mice was evaluated daily. The disease activity index (DAI) was used to assess the mice daily as previously described (23); DAI=[(score of weight loss rate) + (score of stool consistency) + (score of hematochezia)]/3.

Humane endpoint criteria for all experiments that involved mice were assessed daily. Euthanasia was performed when mice exhibited signs of distress, such as weight loss after treatment ≥25%, hunched posture or loss of active movements. Animals with diarrhea, but weight loss <25%, received daily i.p. injections of saline (1 ml three times at 8-h intervals) to avoid dehydration as previously described (24). Animals were euthanized using an overdose of pentobarbital (i.p.; 150 mg/kg supplemented as required) (25). The loss of pedal withdrawal reflexes, and the cessation of respiration and heartbeat for 6 min in mice were used to confirm that they were dead. No mice died during the experiment.

Histological analysis and immunohistochemistry. Hematoxylin and eosin (H&E) staining was performed to assess the induction of IBD. After being euthanized, the colon tissues from normal and IBD mice were collected and fixed in 4% paraformaldehyde for 24 h at 37˚C. The tissues were then embedded using paraffin and were sectioned (thickness, 6 μm) using an SM2500 microtome (Leica Microsystems GmbH). The sections were stained using H&E for 10 min at 37˚C according to a standard protocol. For immunohistochemistry, unstained 4-mm sections were cut from paraffin blocks and incubated at 65˚C for 30 min. The slides were deparaffinized in xylene followed by absolute ethanol and subsequent rehydration in graded ethanol. Antigen retrieval was performed by immersing slides in boiling citric acid buffer (pH 6.0) for 15 min. Following blocking of endogenous peroxidase activity for 20 min in 3% hydrogen peroxide at room temperature, the sections were incubated with the following primary antibodies for 1 h at room temperature: Occludin (1:200; cat. no. 27260-1-AP; ProteinTech Group, Inc.), zonula occludens-1 (ZO-1; 1:200; cat. no. ab216880; Abcam) and claudin-2 (1:200; cat. no. ab53032; Abcam). Subsequently, after three washes with PBS, the sections were incubated with HRP-conjugated goat anti-rabbit IgG H&L (1:1,000; cat. no. ab6721; Abcam) secondary antibodies at 37˚C for 10 min. Sections were incubated with the strept-ABC complex reagent for 15 min, and subsequently exposed to 3,3'-diaminobenzidine, counterstained with hematoxylin and assessed using a confocal microscope (Olympus Corporation).

Measurement of malondialdehyde (MDA), superoxide dismutase (SOD), catalase (CAT) and glutathione (GSH) levels. MDA, SOD, CAT and GSH in colon tissues were assessed using the Lipid Oxidation MDA Assay kit (cat. no. S0131S; Beyotime Institute of Biotechnology), Total SOD Assay kit (cat. no. S0101S; Beyotime Institute of Biotechnology), CAT Detection kit (cat. no. S0051; Beyotime Institute of Biotechnology) and Total GSH Assay kit (cat. no. S0052; Beyotime Institute of Biotechnology), respectively. All procedures were performed according to the manufacturer's protocols. The GSH content, and the activities of MDA, SOD and CAT were normalized to the corresponding total protein content.

TUNEL assay. Paraffin-embedded colon sections were stained using a TUNEL assay kit (Roche Diagnostics) at 37˚C for 1 h and counterstained with 2 μg/ml DAPI at room temperature for 10 min. Mouse colon tissues were fixed in 4% paraformaldehyde at room temperature for 24 h. Then, the colon tissues were cut into 5-μm thick tissue sections which were treated with 0.1% Triton X-100 for 15 min (cat. no. X10010; Shanghai Angyi Biotechnology Co., Ltd.) before staining. The apoptotic cells were quantified by counting the number of positive cells in four fields with at least 400 cells per field in each group. The apoptotic cells were assessed using a fluorescence microscope (Olympus Corporation).

Western blotting. Caco-2 cell samples and mouse colon tissues were collected and lysed using RIPA lysis buffer containing protease inhibitor (cat. no. P0013C; Beyotime Institute of Biotechnology). The protein concentration was assessed using a BCA protein assay kit (cat. no. P0012; Beyotime Institute of Biotechnology). The protein samples (30 μg/lane) were then separated by SDS-PAGE on 8-15% gels. The proteins were transferred onto nitrocellulose membranes, which were blocked in 5% skimmed milk for 2 h at room temperature and incubated with the following specific primary antibodies overnight at 4˚C: Occludin (1:3,000; cat. no. 27260-1-AP; ProteinTech Group, Inc.), ZO-1 (1:5,000; cat. no. 21773-1-AP; ProteinTech Group, Inc.), claudin-2 (1:500; cat. no. ab53032; Abcam), Bcl-2 (1:5,000; cat. no. 12789-1-AP; ProteinTech Group, Inc.), Bax (1:5,000; cat. no. 50599-2-Ig; ProteinTech Group, Inc.), cleaved caspase-3 (1:500; cat. no. ab32042; Abcam), caspase-3 (1:5,000; cat. no. ab32351; Abcam), heme oxygenase-1 (HO-1; 1:1,500; cat. no. 10701-1-AP; ProteinTech Group, Inc.), high mobility group box 1 protein (HMGB1; 1:1,500; cat. no. 10829-1-AP; ProteinTech Group, Inc.) and GAPDH (1:2,500; cat. no. ab9485; Abcam). Then, the membranes were incubated with HRP-conjugated goat anti-rabbit IgG H&L (1:3,000; cat. no. ab6721; Abcam) secondary antibodies at room temperature for 1 h. The membranes were washed using TBS with 0.05% Tween-20 three times and the protein levels were assessed using the BeyoECL Star kit (cat. no. P0018AS; Beyotime Institute of

Biotechnology). Signals were quantified using ImageJ software (version 1.47; National Institutes of Health).

Cell culture. The human colorectal adenocarcinoma Caco-2 cell line with epithelial morphology was purchased from the American Type Culture Collection. Cells were maintained in Dulbecco's Modified Eagle Medium (Gibco; Thermo Fisher Scientific) supplemented with 10% FBS (Gibco; Thermo Fisher Scientific), 100 U/ml penicillin and 100 μg/ml streptomycin at 37˚C under 5% CO_2. When the confluence reached 80% and the cells were highly differentiated, they were treated with 2% DSS or sterilized water (control) for 24 h at 37˚C. In addition, cells were pretreated with ACT (1, 10 and 100 μM) for 6 h at 37˚C. Based on previous reports, the commonly used HO-1 inhibitor tin protoporphyrin (SnPP; 2 μM; Shanghai Aladdin Biochemical Technology Co., Ltd.) was used to pretreat cells for 30 min to inhibit HO-1 expression before ACT treatment (26,27). The experimental grouping of cells was as follows: Control, DSS, DSS + ACT and SnPP + DSS + ACT groups.

MTT assay. The viability of Caco-2 cells was evaluated using an MTT assay kit (Beyotime Institute of Biotechnology) according to the manufacturer's protocol. Briefly, cells were seeded into 96-well plates ($2x10^3$ cells/well) and incubated at 37˚C under 5% CO_2 for 24 h. Subsequently, 20 μl MTT solution was added to the cells for 4 h at 37˚C. The culture medium was carefully removed and 150 μl DMSO was used to dissolve the purple formazan. The absorbance was measured at 570 nm.

ELISA. A total of 50 mg colonic tissues and Caco-2 cells seeded into 96-well plates ($5x10^3$ cells/well) were collected and added to 2-3 ml pre-cooled saline. After homogenization with a glass homogenizer on ice, the tissue was centrifuged at 5,000 x g for 8 min at 4˚C and the supernatant was collected to determine the total protein amount using the BCA method. The concentrations of TNF-α, IL-1β and IL-6 were assessed using the Mouse TNF-α ELISA kit (cat. no. PT512), Human TNF-α ELISA kit (cat. no. PT518), Mouse IL-1β ELISA kit (cat. no. PI301), Human IL-1β ELISA kit (cat. no. PI305), Mouse IL-6 ELISA kit (cat. no. PI326) and Human IL-6 ELISA kit (cat. no. PI330) from Beyotime Institute of Biotechnology, respectively. All procedures were performed according to the manufacturer's protocols.

Bioinformatics and statistical analyses. The potential targets of ACT were assessed using the STITCH website (http://stitch.embl.de; version 5.0), a database of protein-chemical interactions. The data are presented as the mean ± SD and were analyzed using GraphPad Prism 8.0 software (GraphPad Software, Inc.) using one-way ANOVA with Tukey's multiple comparison test. All experiments were repeated at least three times, unless otherwise stated. $P<0.05$ was considered to indicate a statistically significant difference.

Results

ACT inhibits DSS-induced UC in mice. The present study evaluated the potential protective effect of ACT on DSS-induced UC. It was demonstrated that mice displayed slow body weight gain at day 1-4 of DSS treatment and exhibited gradual body weight loss during day 5, 6 and 7 of DSS treatment. Further, 30 or 60 mg/kg ACT treatment significantly elevated the body weight of DSS mice from day 4 onwards (Fig. 1B). DSS-treated mice also demonstrated typical UC characteristics, including significant shortening of the colon (Fig. 1C and D), an acute inflammatory response with mucosal erosion, congestion, edema, reduction of crypts and infiltration of inflammatory cells such as neutrophils (Fig. 1E) and significantly increased DAI (Fig. 1F) compared with in the control group. Compared with the DSS group, DSS-induced colonic shortening was also markedly improved by ACT treatment at 60 mg/kg (Fig. 1C and D). Additionally, mucosal inflammatory cell infiltration, erosion and edema were significantly improved (Fig. 1E) and DAI score was notably decreased (Fig. 1F) in the DSS + 30 mg/kg ACT group and DSS + 60 mg/kg ACT group. These results suggested that UC models were successfully established. Furthermore, these UC-related changes were markedly attenuated by ACT, which suggested that ACT prevented the progression of UC.

ACT inhibits DSS-induced inflammation and oxidative stress in the colon tissues. Consistent with the protective effect of ACT on the progression of UC, DSS significantly increased the levels of inflammatory cytokines, including TNF-α, IL-1β and IL-6, compared with those in the control group, and this was significantly inhibited by 60 mg/kg ACT (Fig. 2A). Furthermore, the levels of oxidative stress markers were assessed. As shown in Fig. 2B, the levels of MDA were significantly increased in the DSS group compared with those in the control group, which suggested that ROS levels were increased in DSS-treated mice. Furthermore, the levels of CAT, GSH and SOD were significantly decreased in the colon of DSS-treated mice compared with those in the control group. As expected, the alterations in MDA, CAT, GSH and SOD were markedly reversed following treatment with 60 mg/kg ACT compared with in the DSS group. These results suggested that ACT inhibited inflammation and oxidative stress in the colon of mice with UC.

ACT prevents DSS-induced colonic barrier dysfunction. The effect of ACT on DSS-induced colonic barrier dysfunction was evaluated. As presented in Fig. 3A and B, immunohistochemistry and western blotting demonstrated that the protein expression levels of occludin and ZO-1, two tight junction proteins, were significantly decreased, whereas claudin-2 protein expression levels were significantly increased in the colon of DSS-treated mice compared with those in the control group. Occludin and ZO-1 expression were noticeably stimulated and claudin-2 expression was markedly inhibited by 60 mg/kg ACT. These results further demonstrated that ACT prevented colonic barrier injury in mice with DSS-induced UC.

ACT inhibits DSS-induced apoptosis in mice colon tissues. To improve the understanding of the mechanism of action of ACT, apoptosis was investigated. As presented in Fig. 4A, the TUNEL assay demonstrated that DSS enhanced the number of TUNEL-positive cells which was then reduced by 40 or 60 mg/kg ACT. Consistently, DSS significantly increased

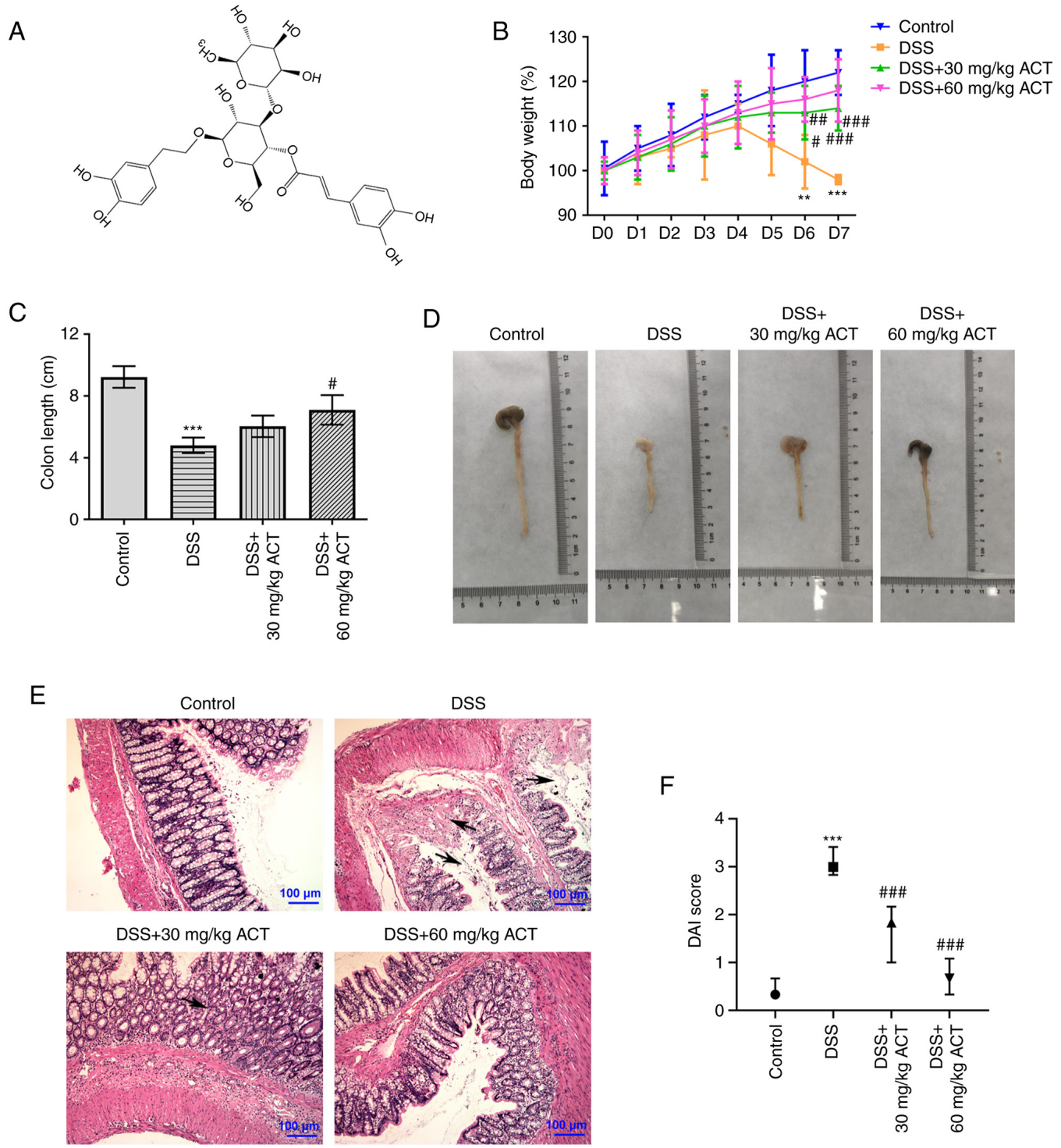

Figure 1. Inhibitory effect of ACT on DSS-induced ulcerative colitis in mice. (A) Chemical structure of ACT. (B) Body weight of mice treated with ACT and DSS. (C and D) Effect of ACT on DSS-induced shortening of the colon. (E) Representative images of the inhibitory effect of ACT on DSS-induced colon injury. The arrows indicate mucosal erosion, reduction of crypts and infiltration of inflammatory cells. (F) Inhibitory effect of ACT on DSS-induced increase of DAI. (n=6). **P<0.01 and ***P<0.001 vs. control; $^{\#}$P<0.05, $^{\#\#}$P<0.01 and $^{\#\#\#}$P<0.001 vs. DSS. ACT, acteoside; DSS, dextran sulphate sodium; DAI, disease activity index.

the expression levels of apoptosis-related proteins, including Bax and cleaved caspase-3/caspase-3, compared with those in the control group, whereas DSS significantly decreased the protein expression levels of Bcl-2 (Fig. 4B). Notably, these changes were markedly altered by pretreatment with 60 mg/kg ACT. These results suggested that ACT inhibited DSS-induced apoptosis.

ACT reverses the effect of DSS on the protein expression levels of HO-1 and HMGB1 in mouse colon tissues. STITCH analysis was subsequently performed to identify the potential binding protein of ACT (http://stitch.embl.de/cgi/network.pl?taskId=TjD9OOCPlkMM) (Fig. 5A). HMGB1 was identified as a potential binding target of ACT. Moreover, it has previously been reported that HMGB1 can be regulated by

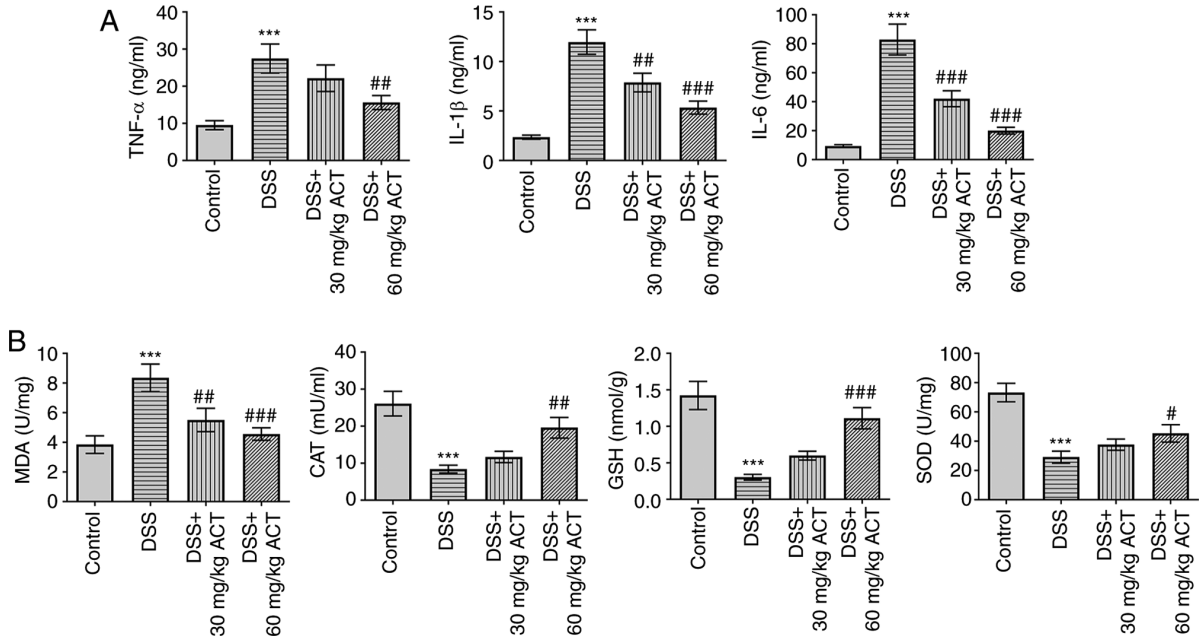

Figure 2. Inhibitory effect of ACT on DSS-induced inflammation of the colon tissues. (A) Inhibitory effect of ACT on DSS-induced levels of inflammatory cytokines, including TNF-α, IL-1β and IL-6, assessed using ELISA. (B) Inhibitory effect of ACT on DSS-induced alterations in the levels of MDA, CAT, GSH and SOD. n=6. ***P<0.001 vs. control; $^{\#}$P<0.05, $^{\#\#}$P<0.01 and $^{\#\#\#}$P<0.001 vs. DSS. ACT, acteoside; DSS, dextran sulphate sodium; MDA, malondialdehyde; CAT, catalase; GSH, glutathione; SOD, superoxide dismutase.

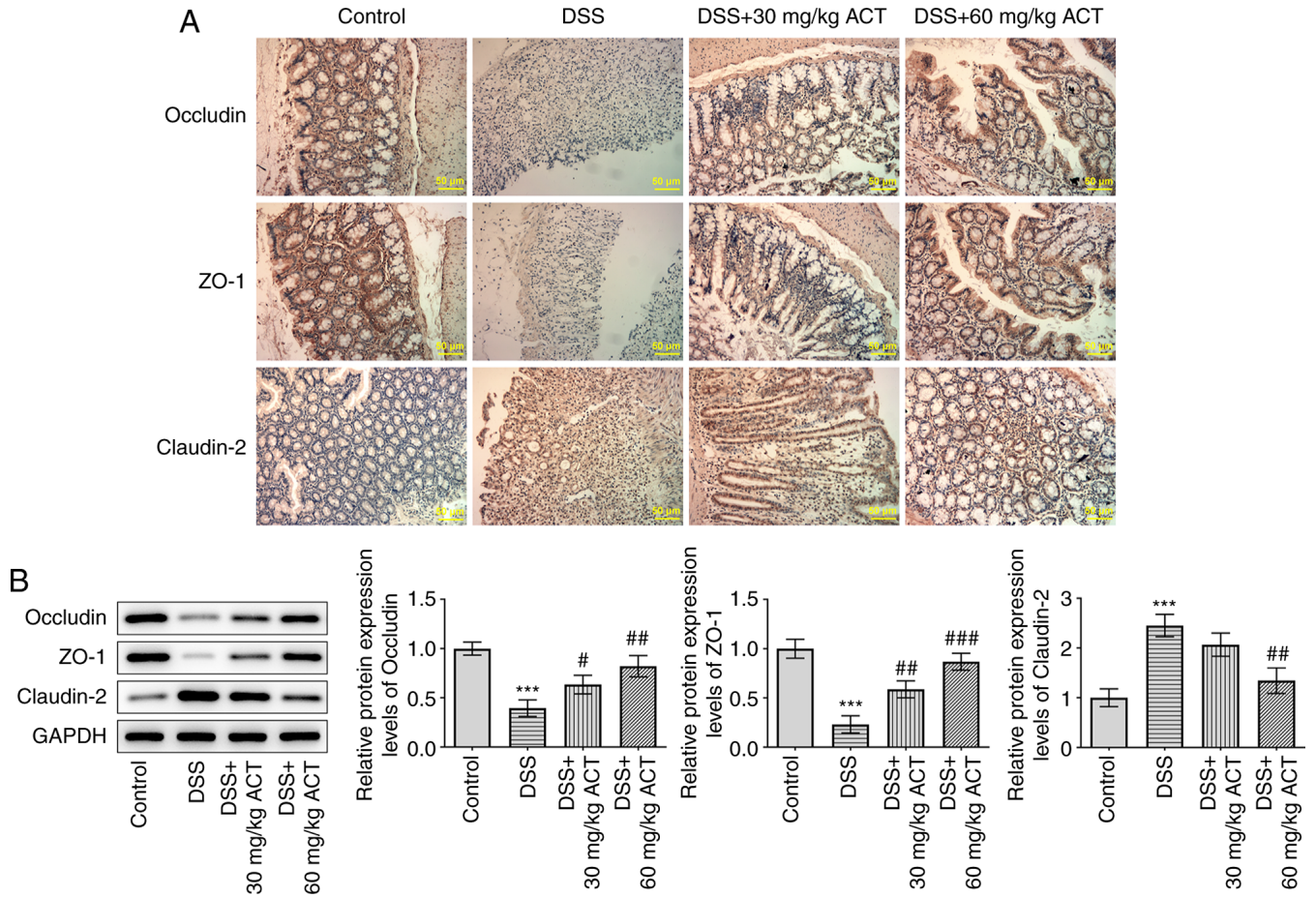

Figure 3. Inhibitory effect of ACT on DSS-induced colonic barrier dysfunction. (A) Representative immunohistochemistry images demonstrating the inhibitory effect of ACT on DSS-induced decreased protein expression levels of occludin and ZO-1, and increased protein expression levels of claudin-2. (B) Representative western blotting images and data demonstrating the inhibitory effect of ACT on DSS-induced decreased protein expression levels of occludin and ZO-1, and increased protein expression levels of claudin-2. n=6. ***P<0.001 vs. control; $^{\#}$P<0.05, $^{\#\#}$P<0.01 and $^{\#\#\#}$P<0.001 vs. DSS. ACT, acteoside; DSS, dextran sulphate sodium; ZO-1, zonula occludens-1.

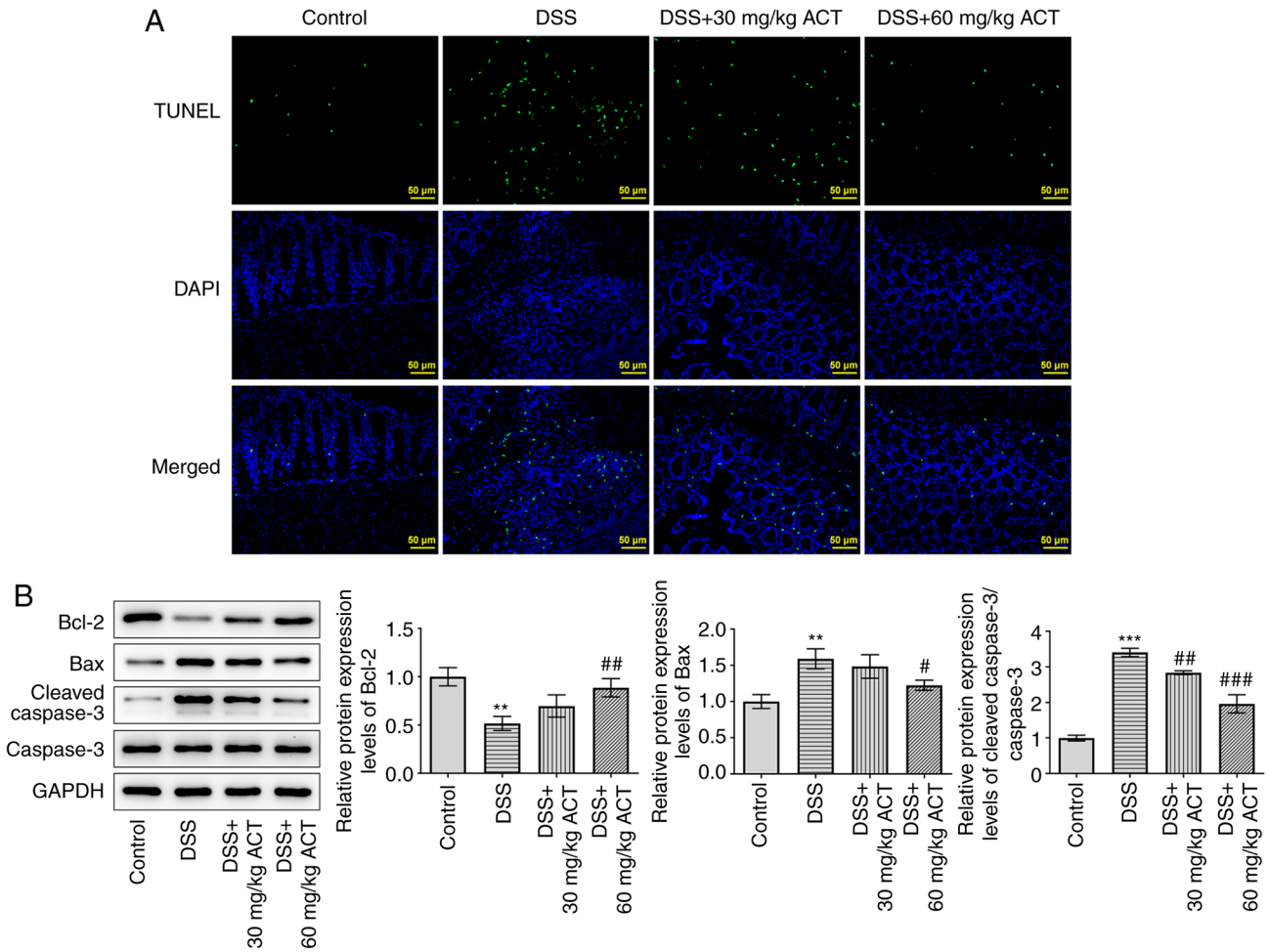

Figure 4. ACT inhibits the DSS-induced apoptosis of mouse tissues. (A) Representative TUNEL images demonstrating the inhibitory effect of ACT on DSS-induced apoptosis. (B) Representative western blotting images demonstrating the effect of ACT on the expression levels of apoptosis-related proteins, including Bcl-2, Bax, cleaved caspase-3 and caspase-3. n=6. **P<0.01 and ***P<0.001 vs. control; $^{\#}$P<0.05, $^{\#\#}$P<0.01 and $^{\#\#\#}$P<0.001 vs. DSS. ACT, acteoside; DSS, dextran sulphate sodium.

HO-1 (28). The present study evaluated the changes in the protein expression levels of HO-1/HMGB1 and the potential effect of ACT on these changes. DSS significantly decreased the protein expression levels of HO-1 compared with those in the control group, whereas it markedly increased HMGB1 protein expression levels (Fig. 5B-D). Notably, the effect of DSS on the altered expression levels of HO-1 and HMGB1 was significantly reversed by 60 mg/kg ACT. These results suggested that ACT may inhibit HMGB1 by promoting HO-1 expression in colon tissues. Therefore, in subsequent experiments, the relationship between ACT and HO-1 was further assessed using the HO-1 inhibitor SnPP.

ACT prevents the DSS-induced decrease of cell viability and inflammation via HMGB1 inhibition in a HO-1-dependent manner in Caco-2 cells. The present study constructed an *in vitro* colon injury model using DSS-induced Caco-2 cells, and a HO-1 inhibitor was used to further study whether the effects of ACT were associated with regulation of the HO-1/HMGB1 signaling pathway. As presented in Fig. 6A, ACT at 1, 10 and 100 μM had no significant effect on the viability of Caco-2 cells compared with that in the control group. However, DSS significantly decreased the viability of Caco-2 cells compared with that in the control group and the inhibitory effect was markedly reversed by ACT in a dose-dependent manner with the most significant effect at 100 μM ACT (Fig. 6B). Therefore, subsequent studies were performed using ACT at a concentration of 100 μM. In addition, DSS significantly increased the levels of inflammatory cytokines, including TNF-α, IL-1β and IL-6, which were markedly inhibited by ACT (Fig. 6C). However, in the presence of SnPP, the inhibitory effect of ACT was markedly reduced. Furthermore, DSS significantly increased MDA levels compared with those in the control group, and significantly decreased the levels of anti-oxidative stress proteins, including CAT, GSH and SOD (Fig. 6D). ACT markedly reversed the effect of DSS on the levels of these four proteins; however, in the presence of SnPP, the inhibitory effects of ACT were markedly reduced (Fig. 6D). These results were consistent with those of the *in vivo* study (Fig. 2B) and demonstrated that the addition of the HO-1 inhibitor effectively reversed the effects of ACT.

ACT prevents DSS-induced cell injury and alterations of apoptosis-related proteins through HMGB1 inhibition in a HO-1-dependent manner in Caco-2 cells. Besides inflammation, the present study evaluated the effect of ACT on DSS-induced cell injury and apoptosis in Caco-2 cells.

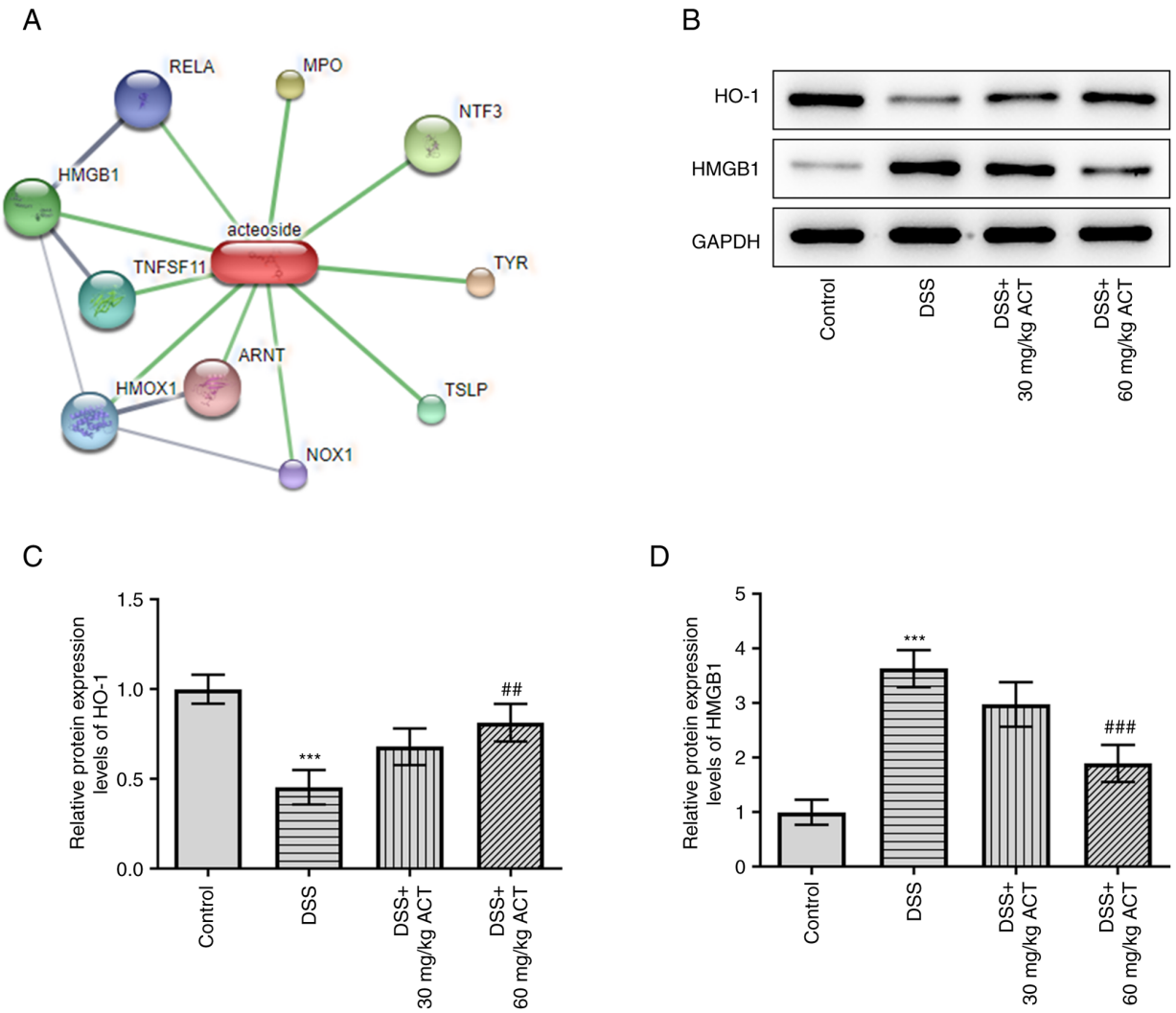

Figure 5. ACT reverses the effect of DSS on the expression of HO-1 and HMGB1 in mice colon tissues. (A) The potential binding protein of ACT. (B) Representative western blot images of HO-1 and HMGB1 protein expression levels. (C) Effect of ACT on DSS-induced reduction of HO-1 protein expression levels. (D) Effect of ACT on the DSS-induced protein expression levels of HMGB1. n=6; ***P<0.001 vs. control; $^{\#\#}$P<0.01 and $^{\#\#\#}$P<0.001 vs. DSS. ACT, acteoside; DSS, dextran sulphate sodium; HO-1, heme oxygenase-1; HMGB1, high mobility group box 1 protein.

As presented in Fig. 7A, DSS significantly decreased the protein expression levels of occludin and ZO-1, and significantly increased the protein expression levels of claudin-2 compared with those in the control group. Pretreatment with ACT significantly inhibited the effects of DSS and the inhibitory effect of ACT was markedly reduced in the presence of SnPP. In addition, DSS significantly increased the expression levels of apoptosis-related proteins, including Bax and cleaved caspase-3, whereas DSS significantly decreased the protein expression levels of Bcl-2 compared with those in the control group (Fig. 7B). These changes were significantly reversed by pretreatment with ACT compared with in the DSS group. However, in the presence of SnPP, the effect of ACT was significantly reduced compared with that in the DSS + ACT group. Finally, the effect of ACT on the protein expression levels of HMGB1 was evaluated. DSS significantly increased HMGB1 expression compared with that in the control group, which was significantly inhibited by ACT. The inhibitory effect of ACT was significantly attenuated by SnPP compared with that in the DSS + ACT group. These results suggested that ACT prevented DSS-induced cell injury in a HO-1-dependent manner in Caco-2 cells.

Discussion

An increasing number of studies have reported that ACT inhibits inflammation in osteoarthritis (17), the gastrointestinal tract (19,29) and LPS-induced acute lung injury (18). Therefore, ACT may be considered a promising drug for the treatment of inflammation-related diseases. However, the underlying mechanisms by which ACT exerts its protective effects remain largely unknown. In the present study, research models were constructed using DSS induction, and the effects and mechanisms were assessed using *in vivo* and *in vitro* experiments. The results demonstrated that ACT prevented the progression of UC and colonic barrier dysfunction, and decreased inflammation and oxidative stress.

It has been reported that the degree of oxidative stress, inflammation and apoptosis are aberrantly increased in UC (30). Furthermore, apoptosis serves an important role in the initiation and progression of UC, which is at least partially

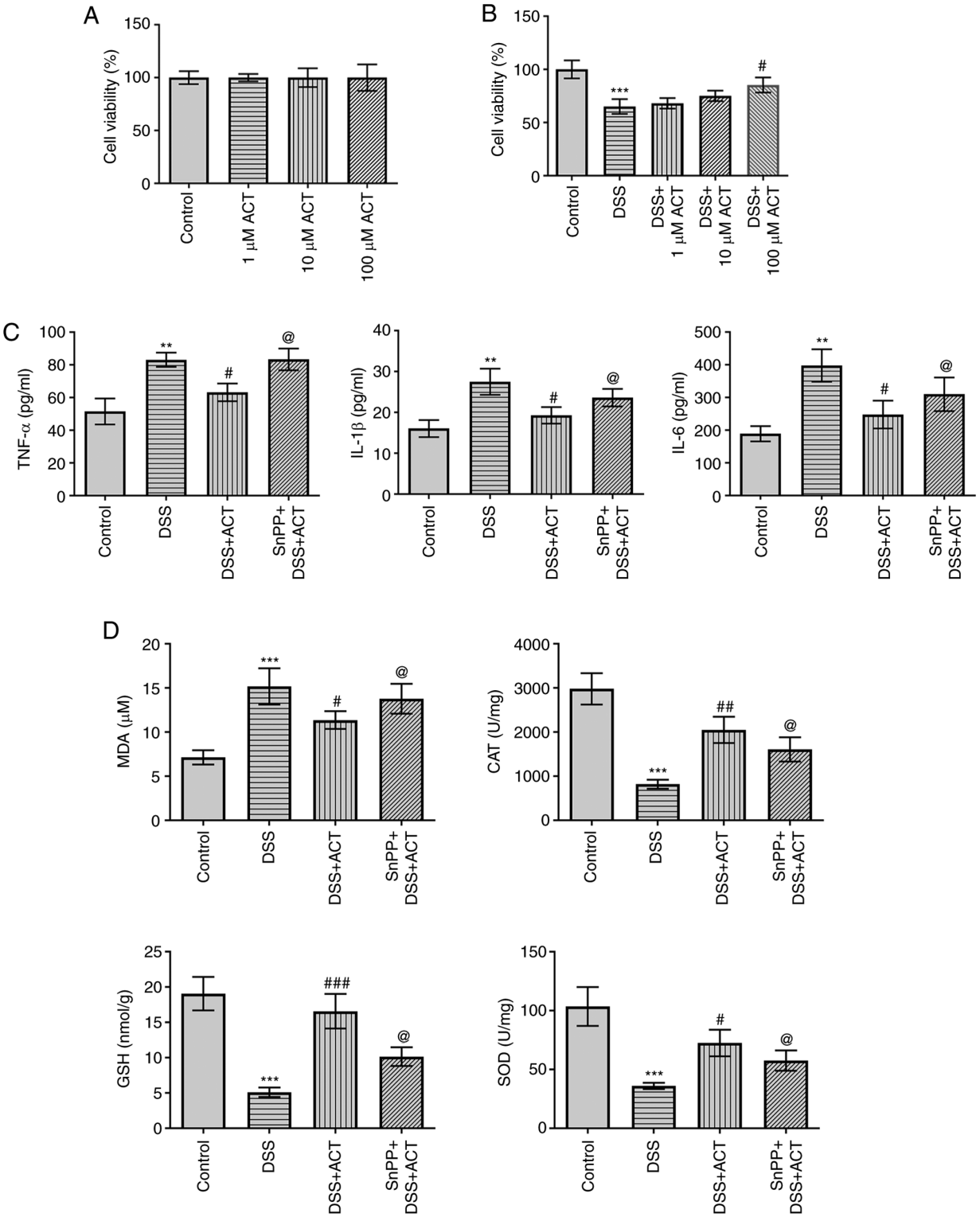

Figure 6. ACT prevents DSS-induced inflammatory response and oxidative stress through high mobility group box 1 protein inhibition via a heme oxygenase-1-dependent manner in Caco-2 cells. (A) ACT demonstrated no significant effect on cell viability in the MTT assay. (B) ACT had a dose-dependent inhibitory effect on the DSS-induced reduction of cell viability. (C) SnPP partially reversed the inhibitory effect of ACT on the DSS-induced production of inflammatory cytokines, including TNF-α, IL-1β and IL-6, in Caco-2 cells. (D) SnPP partially reversed the inhibitory effect of ACT on DSS-induced oxidative stress. n=3. **P<0.01 and ***P<0.001 vs. control; $^{\#}$P<0.05, $^{\#\#}$P<0.01 and $^{\#\#}$P<0.001 vs. DSS; $^{@}$P<0.05 vs. DSS + ACT. ACT, acteoside; DSS, dextran sulphate sodium; MDA, malondialdehyde; CAT, catalase; GSH, glutathione; SOD, superoxide dismutase; SnPP, tin protoporphyrin.

activated by oxidative stress and inflammation (30). In the present study, ACT ameliorated DSS-induced UC injury, while also demonstrating significant inhibitory effects on the inflammatory factors TNF-α, IL-1β and IL-6. Consistent with previous reports (31,32), the present study demonstrated that ACT markedly inhibited DSS-induced oxidative stress and apoptosis. More importantly, high concentrations of ACT (60 mg/kg) significantly increased HO-1 expression and

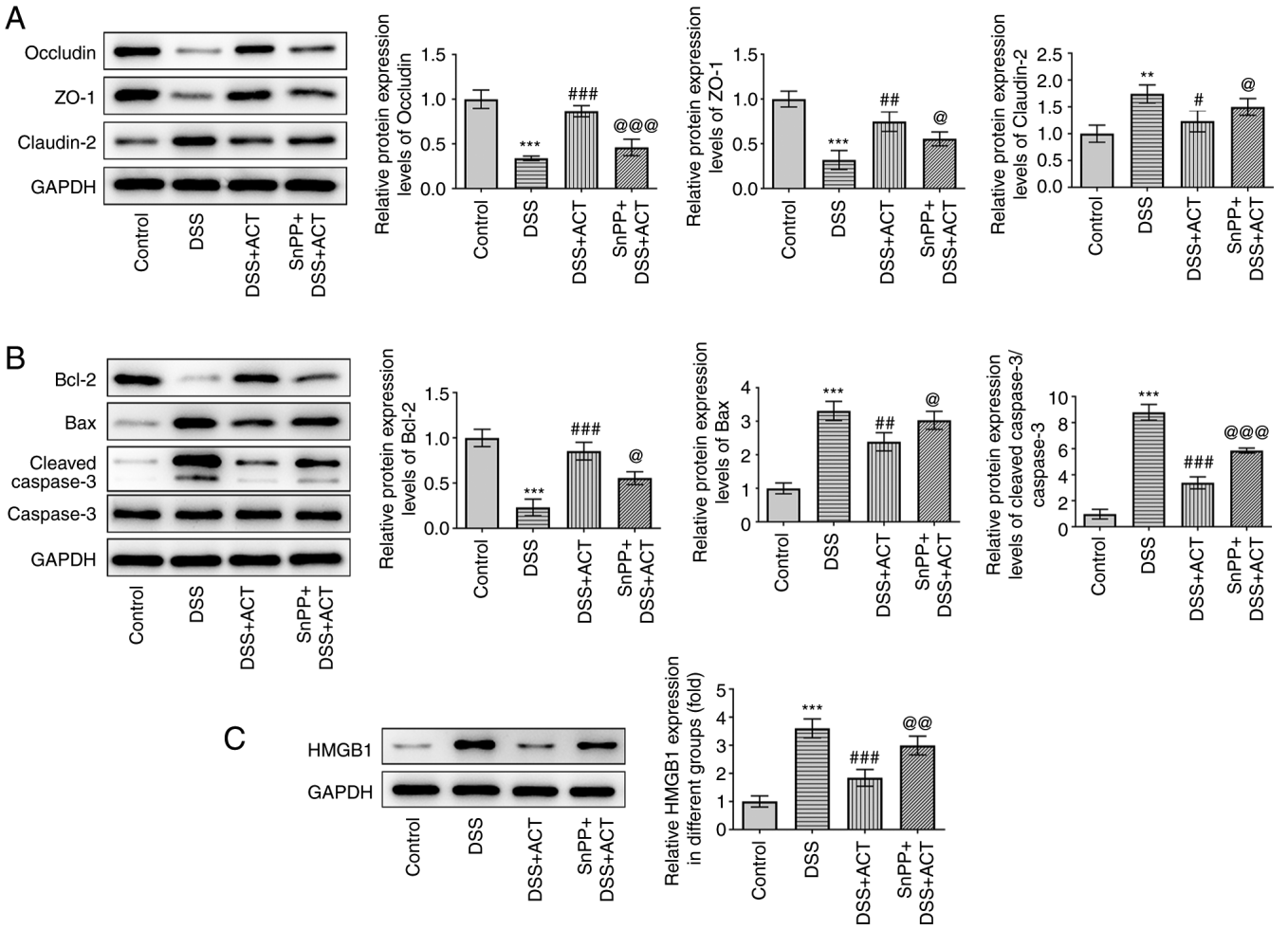

Figure 7. ACT prevents DSS-induced barrier dysfunction and apoptosis through HMGB1 inhibition in a heme oxygenase-1-dependent manner in Caco-2 cells. (A) SnPP partially reversed the inhibitory effect of ACT on DSS-induced changes of tight junction components, including occludin, ZO-1 and claudin-2. (B) SnPP partially reversed the inhibitory effect of ACT on the expression of apoptosis-related proteins, including Bcl-2, Bax, cleaved caspase-3 and caspase-3. (C) Representative western blot images demonstrating the inhibitory effect of ACT on DSS-induced HMGB1 expression with or without SnPP treatment. n=3. **P<0.01 and ***P<0.001 vs. control; $^{\#}$P<0.05, $^{\#\#}$P<0.01 and $^{\#\#\#}$P<0.001 vs. DSS; $^{@}$P<0.05, $^{@@}$P<0.001 and $^{@@@}$P<0.001 vs. DSS + ACT. ACT, acteoside; DSS, dextran sulphate sodium; HMGB1, high mobility group box 1 protein; SnPP, tin protoporphyrin; ZO-1, zonula occludens-1.

inhibited HMGB1 expression compared with those in the DSS group.

An increasing number of studies have reported that HMGB1 serves a critical role in the initiation and progression of UC, and that HMGB1 may be a potential marker for the diagnosis of UC and gut inflammation (33,34). For example, it has been reported that HMGB1 expression is increased in patients with severe UC (35), and that the application of HMGB1 antagonists may provide novel insights into the diagnosis and treatment of UC (36). Consistent with these previous studies, the present study demonstrated that ACT markedly inhibited the increased HMGB1 expression in mice with DSS-induced UC. Considering the central role of HMGB1 in UC, the findings of the present study, that ACT inhibited HMGB1 expression, suggested that ACT may have potential usage in the prevention and treatment of UC.

It has been reported that HO-1 is an upstream regulator of HMGB1 and that gastrodin increases HO-1 expression, leading to inhibition of HMGB1 and NF-κB in Tourette syndrome (37). Wang *et al* (38) reported that HO-1 inducers (hemin and cobalt protoporphyrin IX) or transfection with HO-1 markedly inhibited LPS-induced HMGB1 release and translocation of HMGB1 from the nucleus to the cytosol in RAW264.7 cells, a monocyte/macrophage like cell lineage. Further *in vivo* study demonstrated that HO-1 inducers improved the survival of mice in a LPS- and cecal ligation and puncture-induced sepsis model (38). In the present study, the effects of ACT were interfered with using the HO-1 inhibitor SnPP. Consistent with the previous reports, the results of the present study demonstrated that ACT significantly decreased the protein expression levels of HMGB1 via the activation of HO-1.

In conclusion, the present study demonstrated that ACT protected against the progression of UC. Notably, it was suggested that the molecular mechanism by which ACT may exert its protective effect was via the inhibition of HMGB1 in a HO-1-dependent manner. This finding may provide the fundamental basis for the potential clinical usage of this component in the treatment of UC.

Acknowledgements

Not applicable.

Funding

The present study was supported by the Beijing Natural Science Foundation (grant no. 7204303).

Availability of data and materials

The datasets used and/or analyzed during the current study are available from the corresponding author on reasonable request.

Authors' contributions

WG, XW, FL, SC, SW and SD conceived and designed the study, and acquired and interpreted the data. WG, XW, QZ, LY and FL performed the experiments. SC, SW, QZ and LY wrote the manuscript. WG, XW, FL, SC and SD confirm the authenticity of all the raw data. All authors read and approved the final manuscript.

Ethics approval and consent to participate

All animal experiments were performed according to the Institutional Guidelines for the Care and Use of Laboratory Animals in Research and were approved by the Biomedical Ethics Committee of Peking University (approval no. LA2020356).

Patient consent for publication

Not applicable.

Competing interests

The authors declare that they have no competing interests.

References

1. Hodson R: Inflammatory bowel disease. Nature 540: S97, 2016.
2. Chu H, Khosravi A, Kusumawardhani IP, Kwon AH, Vasconcelos AC, Cunha LD, Mayer AE, Shen Y, Wu WL, Kambal A, *et al*: Gene-microbiota interactions contribute to the pathogenesis of inflammatory bowel disease. Science 352: 1116-1120, 2016.
3. Neurath MF: Cytokines in inflammatory bowel disease. Nat Rev Immunol 14: 329-342, 2014.
4. Zhang YZ and Li YY: Inflammatory bowel disease: Pathogenesis. World J Gastroenterol 20: 91-99, 2014.
5. Ungar B and Kopylov U: Advances in the development of new biologics in inflammatory bowel disease. Ann Gastroenterol 29: 243-248, 2016.
6. Ng SC, Tang W, Ching JY, Wong M, Chow CM, Hui AJ, Wong TC, Leung VK, Tsang SW, Yu HH, *et al*: Incidence and phenotype of inflammatory bowel disease based on results from the Asia-pacific Crohn's and colitis epidemiology study. Gastroenterology 145: 158-165.e152, 2013.
7. Kaser A, Zeissig S and Blumberg RS: Inflammatory bowel disease. Annu Rev Immunol 28: 573-621, 2010.
8. Maloy KJ and Powrie F: Intestinal homeostasis and its breakdown in inflammatory bowel disease. Nature 474: 298-306, 2011.
9. Cho JH: The genetics and immunopathogenesis of inflammatory bowel disease. Nat Rev Immunol 8: 458-466, 2008.
10. Khor B, Gardet A and Xavier RJ: Genetics and pathogenesis of inflammatory bowel disease. Nature 474: 307-317, 2011.
11. Wang R, Luo Y, Lu Y, Wang D, Wang T, Pu W and Wang Y: Maggot extracts alleviate inflammation and oxidative stress in acute experimental colitis via the activation of Nrf2. Oxid Med Cell Longev 2019: 4703253, 2019.
12. Saito M, Chen-Yoshikawa TF, Suetsugu K, Okabe R, Takahagi A, Masuda S and Date H: Pirfenidone alleviates lung ischemia-reperfusion injury in a rat model. J Thorac Cardiovasc Surg 158: 289-296, 2019.
13. Wang Y, Shou Z, Fan H, Xu M, Chen Q, Tang Q, Liu X, Wu H, Zhang M, Yu T, *et al*: Protective effects of oxymatrine against DSS-induced acute intestinal inflammation in mice via blocking the RhoA/ROCK signaling pathway. Biosci Rep: Jul 18, 2019 (Epub ahead of print).
14. Wu X, He W, Zhang H, Li Y, Liu Z and He Z: Acteoside: A lipase inhibitor from the Chinese tea Ligustrum purpurascens kudingcha. Food Chem 142: 306-310, 2014.
15. Esposito E, Mazzon E, Paterniti I, Dal Toso R, Pressi G, Caminiti R and Cuzzocrea S: PPAR-alpha contributes to the anti-inflammatory activity of verbascoside in a model of inflammatory bowel disease in mice. PPAR Res 2010: 917312, 2010.
16. Gao H, Cui Y, Kang N, Liu X, Liu Y, Zou Y, Zhang Z, Li X, Yang S, Li J, *et al*: Isoacteoside, a dihydroxyphenylethyl glycoside, exhibits anti-inflammatory effects through blocking toll-like receptor 4 dimerization. Br J Pharmacol 174: 2880-2896, 2017.
17. Qiao Z, Tang J, Wu W, Tang J and Liu M: Acteoside inhibits inflammatory response via JAK/STAT signaling pathway in osteoarthritic rats. BMC Complement Altern Med 19: 264, 2019.
18. Jing W, Chunhua M and Shumin W: Effects of acteoside on lipopolysaccharide-induced inflammation in acute lung injury via regulation of NF-kappaB pathway in vivo and in vitro. Toxicol Appl Pharmacol 285: 128-135, 2015.
19. Hausmann M, Obermeier F, Paper DH, Balan K, Dunger N, Menzel K, Falk W, Schoelmerich J, Herfarth H and Rogler G: In vivo treatment with the herbal phenylethanoid acteoside ameliorates intestinal inflammation in dextran sulphate sodium-induced colitis. Clin Exp Immunol 148: 373-381, 2007.
20. Committee for the Update of the Guide for the Care and Use of Laboratory Animals: Guide for the Care and Use of Laboratory Animals. 8th edition. The National Academies Press, Washington, DC, 2011.
21. Liu YJ, Tang B, Wang FC, Tang L, Lei YY, Luo Y, Huang SJ, Yang M, Wu LY, Wang W, *et al*: Parthenolide ameliorates colon inflammation through regulating Treg/Th17 balance in a gut microbiota-dependent manner. Theranostics 10: 5225-5241, 2020.
22. Eichele DD and Kharbanda KK: Dextran sodium sulfate colitis murine model: An indispensable tool for advancing our understanding of inflammatory bowel diseases pathogenesis. World J Gastroenterol 23: 6016-6029, 2017.
23. Park YH, Kim N, Shim YK, Choi YJ, Nam RH, Choi YJ, Ham MH, Suh JH, Lee SM, Lee CM, *et al*: Adequate dextran sodium sulfate-induced colitis model in mice and effective outcome measurement method. J Cancer Prev 20: 260-267, 2015.
24. Chen Z, Yu K, Zhu F and Gorczynski R: Over-expression of CD200 protects mice from dextran sodium sulfate induced colitis. PLoS One 11: e0146681, 2016.
25. Dutton JW III, Artwohl JE, Huang X and Fortman JD: Assessment of pain associated with the injection of sodium pentobarbital in laboratory mice (mus musculus). J Am Assoc Lab Anim Sci 58: 373-379, 2019.
26. Ren J, Su D, Li L, Cai H, Zhang M, Zhai J, Li M, Wu X and Hu K: Anti-inflammatory effects of aureusidin in LPS-stimulated RAW264.7 macrophages via suppressing NF-κB and activating ROS- and MAPKs-dependent Nrf2/HO-1 signaling pathways. Toxicol Appl Pharmacol 387: 114846, 2020.
27. Lien GS, Wu MS, Bien MY, Chen CH, Lin CH and Chen BC: Epidermal growth factor stimulates nuclear factor-κB activation and heme oxygenase-1 expression via c-Src, NADPH oxidase, PI3K, and Akt in human colon cancer cells. PLoS One 9: e104891, 2014.
28. Tsoyi K, Lee TY, Lee YS, Kim HJ, Seo HG, Lee JH and Chang KC: Heme-oxygenase-1 induction and carbon monoxide-releasing molecule inhibit lipopolysaccharide (LPS)-induced high-mobility group box 1 release in vitro and improve survival of mice in LPS- and cecal ligation and puncture-induced sepsis model in vivo. Mol Pharmacol 76: 173-182, 2009.
29. Reinke D, Kritas S, Polychronopoulos P, Skaltsounis AL, Aligiannis N and Tran CD: Herbal substance, acteoside, alleviates intestinal mucositis in mice. Gastroenterol Res Pract 2015: 327872, 2015.
30. Tian T, Wang Z and Zhang J: Pathomechanisms of oxidative stress in inflammatory bowel disease and potential antioxidant therapies. Oxid Med Cell Longev 2017: 4535194, 2017.

31. Xia D, Zhang Z and Zhao Y. Acteoside attenuates oxidative stress and neuronal apoptosis in rats with focal cerebral ischemia-reperfusion injury. Biol Pharm Bull 41: 1645-1651, 2018.
32. Peerzada KJ, Faridi AH, Sharma L, Bhardwaj SC, Satti NK, Shashi B and Tasduq SA: Acteoside-mediates chemoprevention of experimental liver carcinogenesis through STAT-3 regulated oxidative stress and apoptosis. Environ Toxicol 31: 782-798, 2016.
33. Nakov R: New markers in ulcerative colitis. Clin Chim Acta 497: 141-146, 2019.
34. Palone F, Vitali R, Cucchiara S, Pierdomenico M, Negroni A, Aloi M, Nuti F, Felice C, Armuzzi A and Stronati L: Role of HMGB1 as a suitable biomarker of subclinical intestinal inflammation and mucosal healing in patients with inflammatory bowel disease. Inflamm Bowel Dis 20: 1448-1457, 2014.
35. Chen Y, Wu D and Sun L: Clinical significance of high-mobility group box 1 protein (HMGB1) and Nod-like receptor protein 3 (NLRP3) in patients with ulcerative colitis. Med Sci Monit 26: e919530, 2020.
36. Hu Z, Wang X, Gong L, Wu G, Peng X and Tang X: Role of high-mobility group box 1 protein in inflammatory bowel disease. Inflamm Res 64: 557-563, 2015.
37. Long H, Ruan J, Zhang M, Wang C and Huang Y: Gastrodin alleviates Tourette syndrome via Nrf-2/HO-1/HMGB1/NF-small ka, CyrillicB pathway. J Biochem Mol Toxicol 33: e22389, 2019.
38. Wang J, Hu X, Xie J, Xu W and Jiang H: Beta-1-adrenergic receptors mediate Nrf2-HO-1-HMGB1 axis regulation to attenuate hypoxia/reoxygenation-induced cardiomyocytes injury in vitro. Cell Physiol Biochem 35: 767-777, 2015.